Journal of Thermal Analysis and Calorimetry, Vol. 88 (2007) 3, 833–841

EFFECT OF POLY(BISPHENOL A ACRYLOXYETHYL PHOSPHATE) ON THE ACTIVATION ENERGY IN THERMAL DEGRADATION OF URETHANE ACRYLATE

*Z.-G. Huang and W.-F. Shi**

State Key Laboratory of Fire Science and Department of Polymer Science and Engineering, University of Science and Technology of China, Hefei, Anhui 230026, P.R. China

Poly(bisphenol A acryloxyethyl phosphate) (BPAAEP) was blended in different ratios with a commercial urethane acrylate to obtain a series of UV curable flame-retardant resins. The thermal oxidative degradation mechanism of their cured films in air were studied by thermogravimetric analysis at several heating rates between 5 and 20°C min^{-1}. The activation energies were determined using Kissinger method, Friedman method, Flynn–Wall method, Horowitz–Metzger method and Ozawa method. The results showed that the activation energies of the blends were lower than that of pure urethane acrylate at lower degree of degradation, whereas the higher activation energies were obtained at higher degree of degradation.

Keywords: *activation energy, degradation kinetics, flame-retardant, phosphate, UV curable*

Introduction

UV curing technology has been widely used in the fields of protective coatings, electronics, adhesives and inks due to its high cure speed, energy conservation, pollution reduction and cost-effectiveness [1]. As well known, urethane acrylates are widely used in various UV coating industries because of their favorable properties with their cured films offering excellent adhesion to most substrates and high flexibility. However, they do not exhibit sufficient flame retardancy and are easily burned. In order to reduce the potential risk in fire incidents, the research in flame retardant material has gained much attention. Therefore, the studies emphasizing the development of technologies to promote flame retardancy and creating flame-retardant materials have increased over several years [2–5]. It has been found that phosphorus-containing monomers and oligomers used as flame-retardants for UV curable systems have several advantages, such as high flame-retardant efficiency, less production of corrosive and toxic gases in flames, and less destruction to the earth's environment [6–9]. Moreover, theses flame-retardant materials also overcome several drawbacks associated with physical blends [10, 11]. The effect of phosphorus-containing flame-retardants was proposed to be via a solid phase mechanism. When burning, they usually form a protective layer of char and poly(phosphoric acid) which inhibits heat and oxygen transfer into the polymer bulk, decreasing the diffusion of combustible gases into the zone of pyrolysis [12–14]. Liu and Lan have found that the investigating degradation mechanism by a thermal decomposition process would provide insight into the flame-retardant effect of a phosphorus-containing polymeric system [15]. However, only a little work has been reported about the kinetics of thermal degradation for phosphorus-containing flame retardant UV curable systems. In our previous work, a UV curable phosphorus-containing oligomer, poly(bisphenol A acryloxyethyl phosphate) (BPAAEP), was synthesized and the thermal degradation behaviour was reported [16, 17].

In this study, BPAAEP was blended with a commercial urethane acrylate, EB220, in different ratios to obtain UV curable flame retardant resins. The thermal oxidative behaviors of their UV cured films were studied by thermogravimetric analysis at different heating rates in air. The overall activation energy was calculated by Kissinger, Friedman and Ozawa methods and the initial mass loss kinetics was emphasized by Horowitz–Metzger and Flynn–Wall methods.

Experimental

Materials

BPAAEP was prepared in our laboratory and the details were described elsewhere [16]. The structure is shown in Fig. 1. EB220, a hexafunctional aromatic urethane acrylate with a molar mass of 1000 g mol^{-1} and viscosity of 28500 cP (25°C), was supplied by UCB Co., Belgium. 2-Hydroxy-2-methyl-1-phenyl-

* Author for correspondence: wfshi@ustc.edu

1388–6150/$20.00

Akadémiai Kiadó, Budapest, Hungary
Springer, Dordrecht, The Netherlands

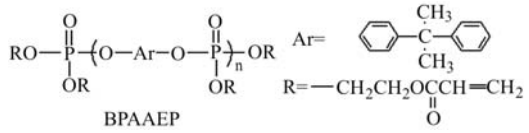

Fig. 1 Molecular structure of BPAAEP

Table 1 Flame retardancy of UV cured EB220, BPAAEP and their blend films

Resin	Formulation/mass%		LOI
	BPAAEP	EB220	
EB220	0	100	25.5
BPAAEP10	10	90	31.0
BPAAEP40	40	60	31.0
BPAAEP	100	0	25.0

1-propanone (Darocur 1173), kindly supplied as a gratis sample by Ciba-Geigy, Switzerland, was used as a photoinitiator. The composition of resins and the flame retardancy of cured films are given in Table 1.

Sample preparation

EB220, BPAAEP and their blends were separately cured with a medium pressure Hg lamp (300 W inch^{-1}, Fusion UV Systems, Inc. USA) in the presence of 3 mass% Darocur 1173.

Methods

Thermogravimetric analysis

The thermogravimetric analysis (TG) was carried out on a Shimadzu TG-50 apparatus under air atmosphere at a purge rate of 20 mL min^{-1}. The heating rates of 5, 10, 15 and 20°C min^{-1} were taken. For each experiment approximately 10.0 mg sample was used in TG test.

Kinetic methods

The methods used for calculating kinetic parameters from TG data are classified into two groups: integral and differential methods. The most suitable method has, however, not yet been clarified [18].

Differential method

The analysis for the changes in thermogravimetric data brought about by variation of the heating rate, β, is the basis of the most powerful differential methods for the determination of kinetic parameters.

- Kissinger method [19, 20] has been used in the literature to determine the activation energies from the plots of logarithm of the heating rates *vs*. the inverse of temperature at the maximum reaction rates (T_{max}) in constant heating rate experiments, using the equation:

$$\ln\left(\frac{\beta}{T_{max}^2}\right)=\left\{\ln\frac{AR}{E}+\ln[n(1-\alpha_{max})^{n-1}]\right\}-\frac{E}{RT_{max}} \quad (1)$$

Therefore, the activation energy can be determined from a plot of $\ln(\beta/T_{max}^2)$ *vs*. $1/T_{max}$.

- Friedman method [21] is probably the most general of the derivative techniques and is based on the comparison of the rates of mass loss α for a given fractional mass loss determined using different linear heating rates β.

This method utilizes the following logarithmic differential equation:

$$\ln\left(\frac{d\alpha}{dt}\right)=\ln A+n\ln(1-\alpha)-\frac{E}{RT} \quad (2)$$

For a constant fractional mass loss the α value at multiple heating rates, by plotting $\ln(d\alpha/dt)$ *vs*. $1/T$ values for activation energy of degradation over a wide range of mass loss could be obtained.

- Flynn–Wall method [22] proposed by Flynn and Wall, is applicable at low conversion (maximum degradation 10%). Differentiation of equation:

$$\frac{d\alpha}{dt}=A(1-\alpha)^n\exp\left(-\frac{E}{RT}\right) \quad (3)$$

with respect to α gives an expression for the slope of the line obtained from a plot of $T^2d\alpha/dT$ *vs*. α.

$$\text{Slope}=\frac{d\left[T^2\left(\frac{d\alpha}{dT}\right)\right]}{d\alpha}=\frac{E}{R}+2T+T^2\left[\frac{f'(\alpha)}{f(\alpha)}\right]\frac{d\alpha}{dT} \quad (4)$$

where $f'(\alpha)$ is the derivative of $f(\alpha)$ with respect to α.

For $\alpha<<1$, the last part of Eq. (4) can be neglected and the slope would be obtained as follows,

$$\text{Slope}=\frac{E}{R}+2T \text{ or } E=R(\text{Slope})-2RT \quad (5)$$

where T is the average temperature at which the slope is taken. The plot of $T^2(d\alpha/dT)$ *vs*. α should give a straight line, from which the activation energy is calculated by using Eq. (5).

Integral methods

- Horowitz–Metzger method [23, 24] calculated the kinetic parameters by one single heating rate TG curve. It simplified the exponential integral, obtaining the following equation

$$\ln[\ln(1-\alpha)^{-1}]=\frac{E\theta}{RT_{max}^2} \quad (6)$$

where θ is the difference between T and T_{max}, T_{max} is the temperature of maximum rate of mass loss. The

activation energy was given by the straight line corresponding to the plot of $\ln[\ln(1-\alpha)^{-1}]$ *vs*. θ.

- Ozawa method [25], which is essentially the same as Flynn and Wall, represents a relatively simply method of determining activation energy directly from mass loss *vs*. temperature data obtained at several heating rates. Equation

$$g(\alpha)=\int_0^{\alpha}\frac{d\alpha}{f(\alpha)}=\frac{A}{\beta}\int_0^{T}\exp\left(-\frac{E}{RT}\right)dT \qquad (7)$$

is integrated using Doyle's approximation, and the result of the integration after taking logarithms was:

$$\log[g(\alpha)]=\log\frac{AE}{R}-\log\beta-2.315-0.4567\frac{E}{RT} \qquad (8)$$

where β, A, E and T have the known meanings, $g(\alpha)$ is the integral function of conversion.

This is one of the integral methods that can determine the activation energy without a knowledge of reaction order. It is used to determine the activation energy for given values of conversion. The activation energies for different conversion values can be calculated from lnβ *vs*. $1/T$ plots.

Results and discussion

Thermal degradation

When flame retardant components are incorporated into polymeric materials, the mass loss pattern of the polymers will be altered [26]. Phosphate groups in the polymer matrices first decomposed at relatively low temperature, and then formed a heat resistant char that retarded the mass loss rate of the polymers at high temperature [27, 28]. Figure 2 shows the TG curves of UV cured EB220 and its blend films with different BPAAEP contents at a constant heating rate of 10°C min^{-1}. It is noted that the cured BPAAEP and BPAAEP40 films exhibit relatively lower thermostability at lower temperature while higher thermostability and higher efficiency in char formation at elevated temperature compared with BPAAEP10 film. Generally speaking, the reduction of initial decomposition temperatures may be attributed to the fact that P–O–C is less stable than common C–C bond. The degraded phosphate group has a big contribution to form compact char to protect the sample from further degradation. As a result, the cured film with high phosphorus content is more stable at high temperature.

Degradation kinetics

Figures 3–6 show the thermal oxidative degradation and DTG curves of the UV cured EB220 and its blend films with different BPAAEP contents corresponding

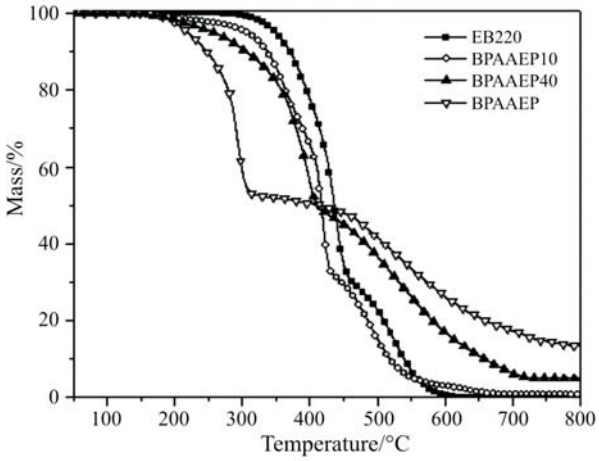

Fig. 2 TG curves of UV cured EB220, BPAAEP and their blend films at the heating rate of 10°C min^{-1}

to the dynamic experiments carried out at different heating rates (5, 10, 15 and 20°C min^{-1}). For all samples, the TG curves are shifted to higher temperatures at higher heating rates, although the shapes of curves are quite similar. Based on the peaks numbers in the DTG curves, the mass loss processes of films are considered as several stages. It can be found that the decomposition of EB220 and BPAAEP takes place at three distinct stages, whereas the decomposition of EB220 blend film with 40 mass% BPAAEP addition takes place at more than three distinct stages besides one prestage for the degradation of P–O–C groups (Table 2). This implies that the decomposition reaction mechanism of EB220 has become more complex after added BPAAEP.

Using Kissinger's Eq. (1), the curves of $\ln(\beta/T_{max}^2)$ *vs*. $1/T_{max}$ for each stage of thermal degradation for UV cured EB220, BPAAEP10, BPAAEP40 and BPAAEP films were plotted, as shown in Fig. 7. The calculated decomposition activation energies are listed in Table 2.

The activation energies for stage 1 and stage 2 in the degradation of phosphorus-containing resins, as

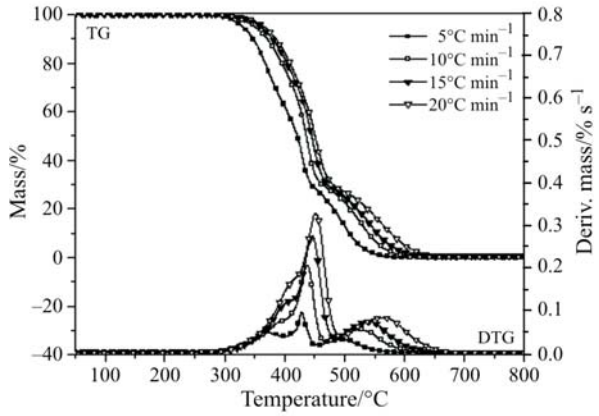

Fig. 3 TG and DTG curves of UV cured EB220 film at different heating rates

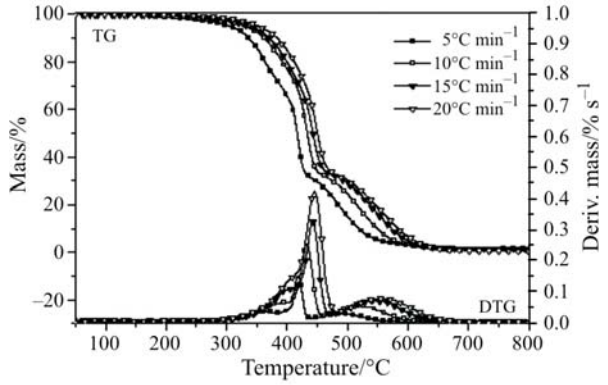

Fig. 4 TG and DTG curves of UV cured BPAAEP10 film at different heating rates

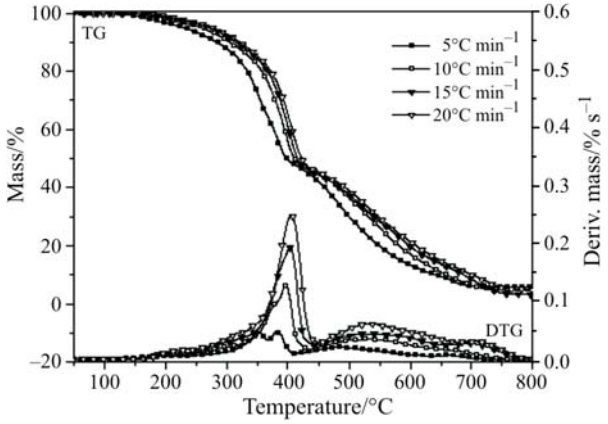

Fig. 5 TG and DTG curves of UV cured BPAAEP40 film at different heating rates

compared with EB220, are found to decrease as the phosphorus content increased. These stages mainly involve the degradation of phosphate and carbonyl groups in the films. Poly(phosphoric acid) as a decomposition product of phosphate further catalyzes the breakage of carbonyl groups, which makes the

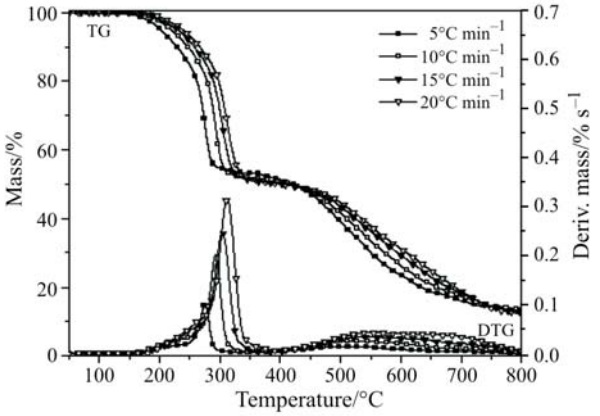

Fig. 6 TG and DTG curves of UV cured BPAAEP films at different heating rates

degradation of carbonyl groups moving to lower temperature and thus the activation energy decreased. However, the mass loss rates at stage 3 are depressed by the incorporation of phosphorus, and thus the activation energies increase with increasing phosphorus contents. This is attributed to the fact that poly(phosphoric acid) can further react with the decomposition product of carbonyl groups to form a complex phosphorus-carbon structure, which is stable at higher temperature. Thus, the activation energies of UV cured EB220 with BPAAEP addition are higher than that of pure EB220 at stage 3.

The activation energy can also be determined using Friedman method by Eq. (2) from a linear fitting of $\ln(d\alpha/dt)$ *vs*. $1/T$ at different conversions. In this study, the conversions of 5, 10, 20, 30, 40, 50, 60, 70, 75, 80 and 90% were chosen. Figure 8 shows the fitting lines for all samples, and the data are listed in Table 3. The activation energies of BPAAEP, BPAAEP40 and BPAAEP10 at 5% conversion are 67.07, 72.75 and 103.80 kJ mol^{-1}, respectively, which are lower than that of pure EB220 (107.71 kJ mol^{-1}). It implies that

Table 2 Calculated degradation activation energies of EB220, BPAAEP and their blend films by Kissinger method

Resin	Region	Conversion α	T_m/°C; β=10°C min^{-1}	E/kJ mol^{-1}	r^a
EB220	stage 1	0.00–0.27	390.36	96.38	0.9985
	stage 2	0.27–0.71	438.13	188.91	0.9987
	stage 3	0.71–1.00	524.3	89.15	0.9983
BPAAEP10	stage 1	0.00–0.26	385.3	90.03	0.9976
	stage 2	0.26–0.68	432.25	184.48	0.9964
	stage 3	0.68–0.98	523.34	98.91	0.9987
BPAAEP40	prestage	0.00–0.02	206.3	78.00	0.9999
	stage 1	0.02–0.15	302.03	95.51	0.9981
	stage 2	0.15–0.32	379.27	84.66	0.9999
	stage 3	0.32–0.53	397.05	169.84	0.9949
	stage 4	0.53–0.95	512.65	160.40	0.9994
BPAAEP	stage 1	0.00–0.16	244.71	73.88	0.9973
	stage 2	0.16–0.48	293.23	93.65	0.9999
	stage 3	0.48–0.86	515.86	163.40	0.9995

[a]correlation coefficient

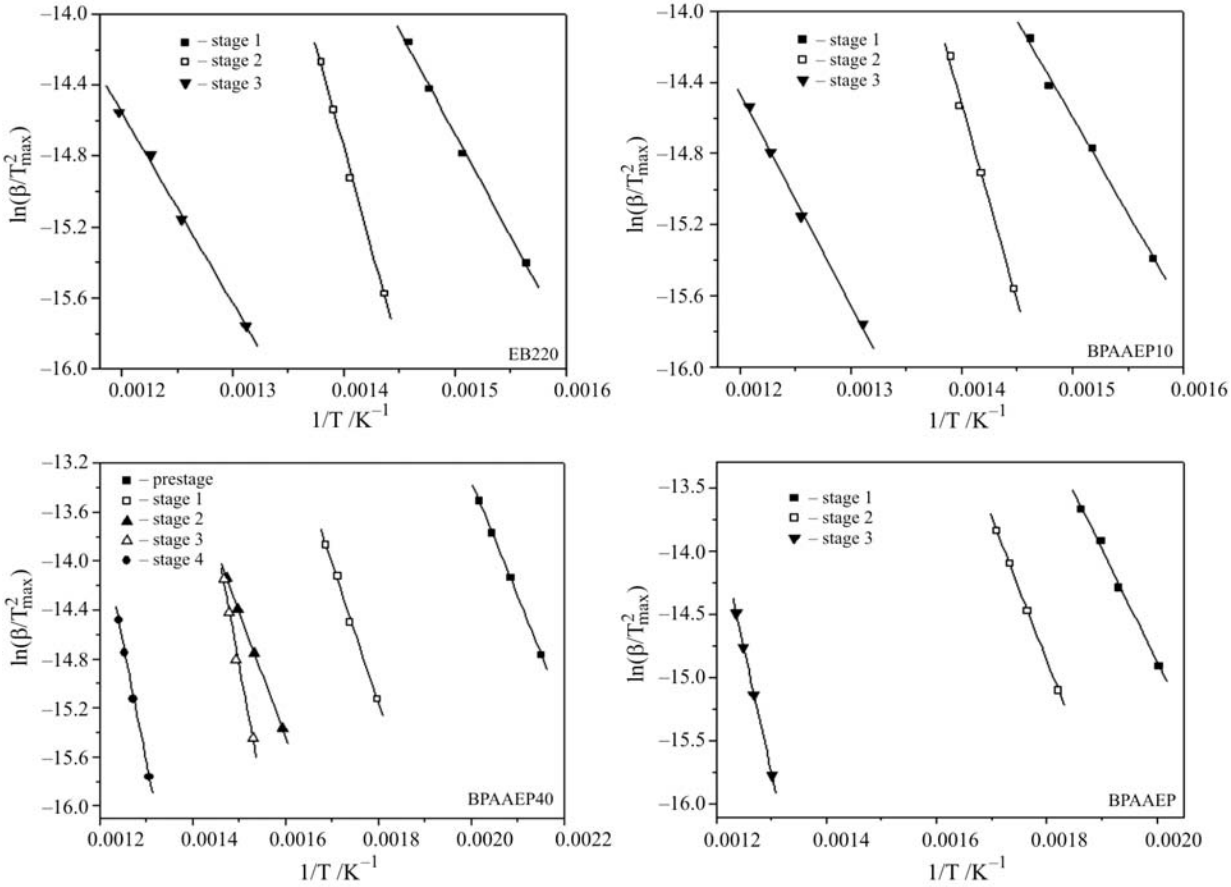

Fig. 7 Plots for degradation activation energies of UV cured EB220, BPAAEP and their films calculated by Kissinger method

the activation energy decreases along with increasing BPAAEP content at 5% conversion. The lower activation energy of this stage is due to the presence of P–O–C structure in the film. It is also coincident with the results obtained from previous FTIR and DP-MS measurements of BPAAEP [17]. It also can be found that the activation energies of BPAAEP, BPAAEP40 and BPAAEP10 are lower than that of EB220 at low conversions, whereas the higher activation energies can be observed at high conversions. This is similar to the results from Kissinger method.

The decomposition rates obtained at the initial stage of mass loss are valuable in UV irradiation-induced degradation kinetics. In many cases, the cured films may lose their desirable properties, such as flexibility and adhesion, during the first few percent of

Table 3 Calculated degradation activation energies of EB220, BPAAEP and their blend films by Friedman method

Conversion α	EB220		BPAAEP10		BPAAEP40		BPAAEP	
	E/kJ mol^{-1}	r^a	E/kJ mol^{-1}	r^a	E/kJ mol^{-1}	r^a	E/kJ mol^{-1}	r^a
0.05	107.71	0.9957	103.80	0.9953	72.75	0.9992	67.07	0.9987
0.10	109.78	0.9948	104.88	0.9982	100.34	0.9995	87.91	0.9985
0.20	113.96	0.9749	111.36	0.9946	108.26	0.9990	106.42	0.9992
0.30	140.42	0.9984	134.75	0.9978	132.36	0.9917	85.61	0.9993
0.40	182.02	1.0000	175.24	0.9966	167.97	0.9991	91.07	0.9986
0.50	189.28	0.9954	147.70	0.9997	–	–	–	–
0.60	163.51	0.9922	117.47	0.9987	138.85	0.9993	142.60	0.9907
0.70	–	–	103.21	0.9991	113.5	0.9962	116.89	0.9925
0.80	90.88	0.9952	93.51	0.9987	116.73	0.9982	208.26	0.9944
0.90	83.16	0.9962	107.97	0.9958	–	–	–	–

[a]correlation coefficient

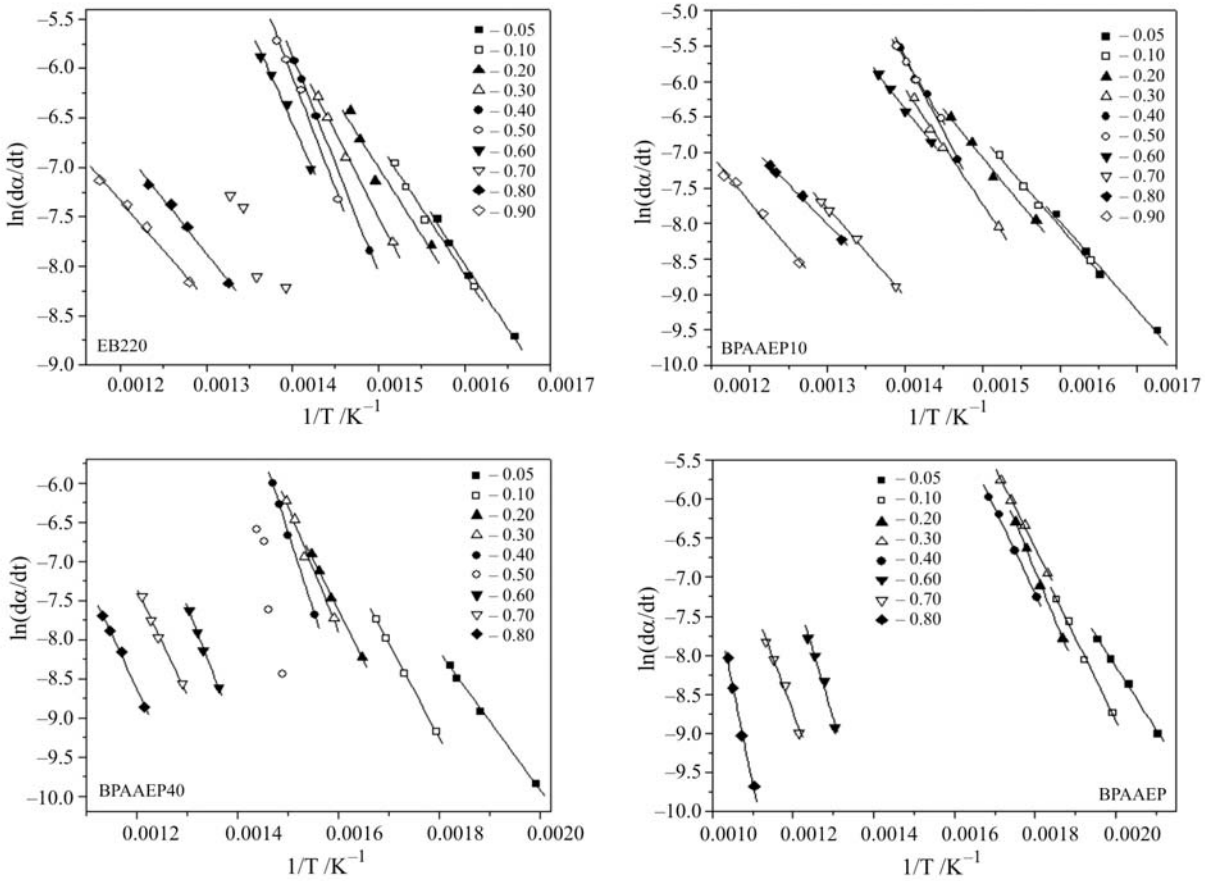

Fig. 8 Plots for degradation activation energies of UV cured EB220, BPAAEP and their blend films at different conversion calculated by Friedman method

mass loss. The activation energies and other kinetic parameters calculated from these early data are thus meaningful in predicting the thermal stability of a polymer. Using Flynn–Wall method by Eq. (5), the curves of $T^2(d\alpha/dT)$ *vs*. α for the initial stage of mass loss (α=0.04~0.06) for all samples were plotted, as shown in Fig. 9. The activation energies calculated from the linear lines are listed in Table 4. It shows a decrease in the activation energy for EB220 with increasing phosphorus content. Using Horowitz–Metzger's integral method by Eq. (6), the activation energies at initial stages (stage 1) of the mass loss are also obtained from the straight lines corresponding to the $\ln[\ln(1-\alpha)^{-1}]$ *vs*. θ (Fig. 10). All the slope data are obtained with good correlation coefficients of higher than 0.99. The calculated activation energy values are listed in Table 4. As can be seen, they have the same tendency to the results from Flynn–Wall's differential method. It has been reported that the thermal degradation of polyurethane begins at the hard segment, since the urethane group is not stable above 230°C [29–31]. As the phosphate groups are located on the hard segments in EB220/BPAAEP blend films after photopolymerized, Grassie and Mackerron have thus concluded that the degradation started at the hard phosphate-containing urethane segments [32]. Therefore, it may be

Table 4 Calculated degradation activation energies of EB220, BPAAEP and their blend films at low conversion by Flynn–Wall and Horowitz–Metzger methods

Resin	Flynn–Wall method (α=0.04~0.06)		Horowitz–Metzger method (stage 1)		
	E/kJ mol^{-1}	r^a	T_{max}/°C	E/kJ mol^{-1}	r^a
EB220	99.17	0.9984	395.38	98.69	0.9994
BPAAEP10	90.81	0.9809	395.36	78.36	0.9994
BPAAEP40	78.95	0.9995	378.26	81.28	1.0000
BPAAEP	66.13	0.9998	244.71	50.17	0.9994

[a]correlation coefficient

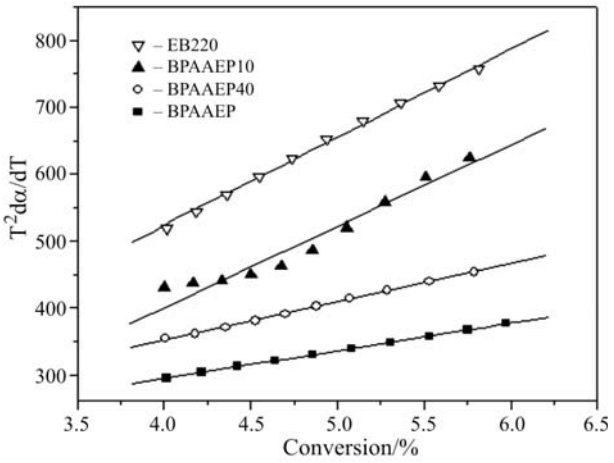

Fig. 9 Dependence of $T^2d\alpha/dT$ on the conversion of EB220, BPAAEP and their blends

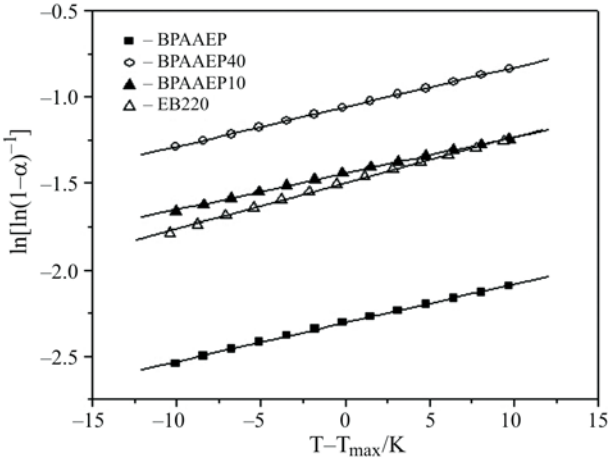

Fig. 10 Plots for degradation activation energies for mass loss of EB220, BPAAEP and their blends in stage 1 by Horowitz–Metzger method

suggested that in segmented polyurethanes, the location of phosphate groups determines where the degradation starts. The low thermal stability of phosphate-containing segments is also reflected in the calculated values of activation energy presented in Table 4, where the activation energy decreases with increasing phosphorus content.

In addition to the differential methods, the activation energy can also be determined using the integral method of Ozawa, Eq. (7) from a linear fitting of lnβ *vs.* $1/T$ at different conversions. For the present work, the conversion values of 5, 10, 20, 30, 40, 50, 60, 70, 80 and 90% were chosen. Figure 11 shows that the fitting lines are nearly parallel, thus indicating the applicability of this method to studied systems in the conversion range investigated. All calculated activation energies are listed in Table 5. The activation energies of BPAAEP, BPAAEP40 and BPAEP10 at 5% conversion are around 75~85 kJ mol^{-1}, whereas that of pure EB220 is 114 kJ mol^{-1}. The decomposition activation energy of about 80 kJ mol^{-1} was also found for phosphate groups in a previous work [33]. The results show that when the conversion reaches to 50% for BPAAEP film, we can not obtain a fitting line, indicating that a complicated reaction mechanism acts at this stage.

The use of a multiple heating rate technique was felt to represent more realistically the variety of heating rates occurred during the pyrolysis and combustion reactions when a polymer burns [34]. However, the activation energies of initial stage of mass loss for all samples show no obviously derivation between the multiple heating rate methods (Kissinger, Friedman and Ozawa method) and single heating rate methods (Flynn–Wall and Horowitz–Metzger method) in this system. This suggests that it is also reasonable to calculate activation energy using Flynn–Wall and Horowitz–Metzger methods at the primary degrada-

Table 5 Calculated degradation activation energies of EB220, BPAAEP and their blend films by Ozawa method

Conversion α	EB220		BPAAEP10		BPAAEP40		BPAAEP	
	E/kJ mol^{-1}	r^a	E/kJ mol^{-1}	r^a	E/kJ mol^{-1}	r^a	E/kJ mol^{-1}	r^a
0.05	114.14	0.9981	85.73	0.9898	81.41	0.9982	73.33	0.9998
0.10	114.98	0.9898	95.26	0.9931	94.21	0.9939	78.96	0.9998
0.20	117.64	0.9929	100.66	0.9892	108.80	0.9878	94.04	0.9996
0.30	135.03	0.9956	123.63	0.9919	117.86	0.9951	95.31	0.9998
0.40	172.23	0.9954	167.42	0.9990	161.90	0.9942	91.97	0.9989
0.50	184.96	0.9998	165.91	0.9998	182.80	0.9984	–	–
0.60	189.06	0.9992	154.51	0.9999	183.15	0.9685	164.00	0.9928
0.70	145.86	0.9987	147.83	0.9968	153.03	0.9859	132.02	0.9948
0.80	108.65	0.9994	115.99	0.9978	130.85	0.9982	166.18	0.9990
0.90	105.94	0.9995	113.68	0.9987	–	–	–	–

[a]correlation coefficient

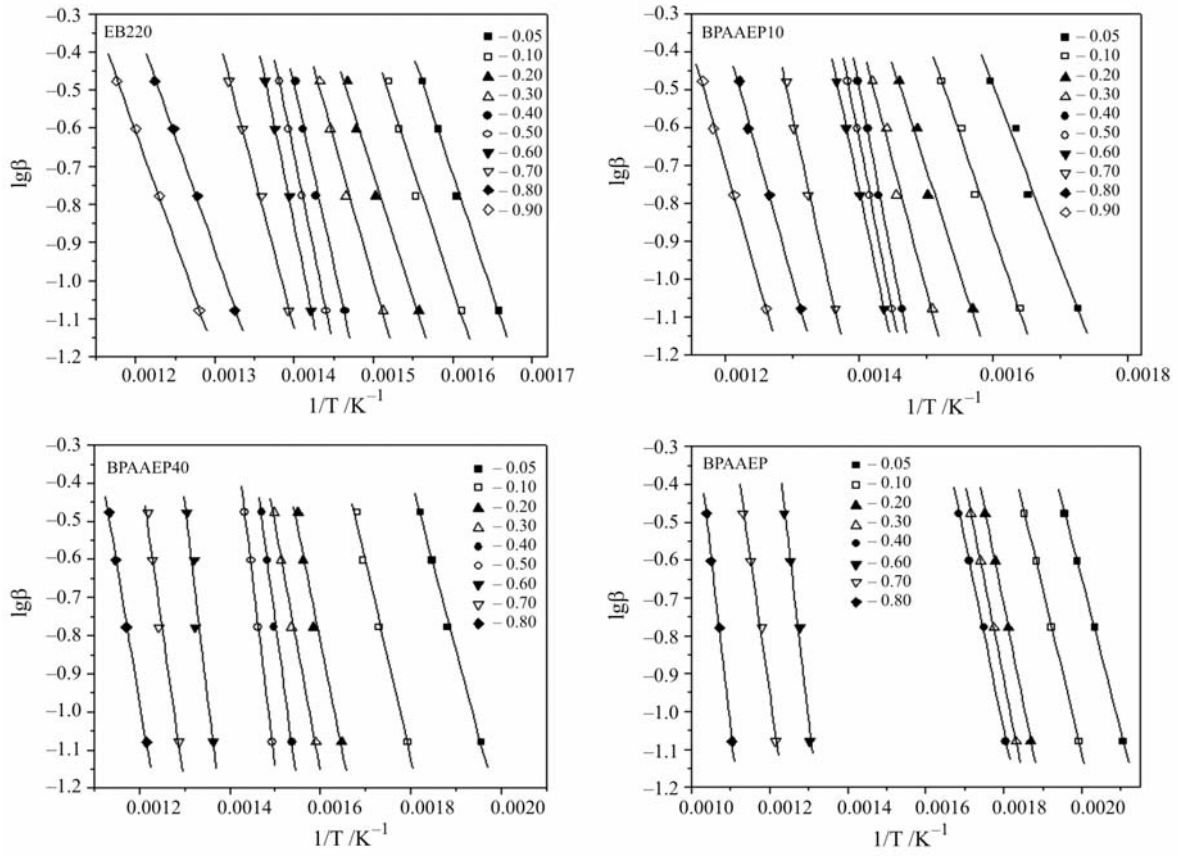

Fig. 11 Plots for degradation activation energies of UV cured EB220, BPAAEP and their blend films at different conversion calculated by Ozawa method

tion stage in this system. Friedman's and Ozawa's calculations are applicable to all points on the TG curves, and Kissinger's method uses only one point, i.e. the point of maximum rate, which is the primary difference from the former two methods. Comparing the decomposition activation energy values of all samples, as calculated via these three methods, they did not show obviously derivation.

Conclusions

From a comparison of the activation energies of EB220 with EB220/BPAAEP at different degradation stages, it can be concluded that the thermal oxidation degradation mechanism of EB220/BPAAEP is greatly changed. P–O–C groups in the cured films could degrade at lower temperature and form poly(phosphoric acid), which catalyzes the degradation of EB220, and further react with the decomposition products of EB220 to form thermally stable compounds on the condensed phase. Thus, as EB220 blended with BPAAEP, the activation energy of thermal degradation at lower conversion decreased, whereas increased afterwards.

Acknowledgements

The authors gratefully acknowledge the financial support of the NKBRSF Project (No. 2001CB409600, China).

References

1 T. Frecska, J. Rad. Curing, 14 (1987) 26.
2 S. W. Zhu and W. F. Shi, Polym. Int., 51 (2002) 223.
3 S. W. Zhu and W. F. Shi, Polym. Int., 53 (2004) 266.
4 J. Ding, H. B. Liang and W. F. Shi, J. Appl. Polym. Sci., 97 (2005) 1776.
5 M. Gao, C. Y. Sun and C. X. Wang, J. Therm. Anal. Cal., 75 (2004) 221.
6 C. S. Wang and J. Y. Shieh, Eur. Polym. J., 36 (2000) 443.
7 D. Avci and A. Z. Albayrak, J. Polym. Sci. Pol. Chem., 41 (2003) 2207.
8 H. B. Liang and W. F. Shi, Polym. Degrad. Stab., 87 (2005) 495.
9 H. B. Liang and W. F. Shi, J. Appl. Polym. Sci., 97 (2005) 185.
10 T. Randoux, J. C. Vanovervelt, B. H. D. Van and G. Camino, Prog. Org. Coat., 45 (2002) 281.
11 K. Mequanint, R. Sanderson and H. Pasch, Polym. Degrad. Stab., 77 (2002) 121.
12 M. Banks, J. R. Ebdon and M. Johnson, Polymer, 34 (1994) 4547.

13 P. J. Davies and A. R. Horrocks, Fire Mater., 24 (2000) 151.
14 S. W. Zhu and W. F. Shi, Polym. Degrad. Stab., 75 (2002) 543.
15 Y. L. Liu, G. H. Hsiue, C. W. Lan and Y. S. Chiu, Polym. Degrad. Stab., 56 (1997) 291.
16 Z. G. Huang and W. F. Shi, Eur. Polym. J., in press.
17 Z. G. Huang and W. F. Shi, Polym. Degrad. Stab., in press.
18 H. Nishizaki, K. Yoshida and J. Wang, J. Appl. Polym. Sci., 25 (1980) 2869.
19 H. E. Kissinger, Anal. Chem., 29 (1957) 1702.
20 M. J. B. Souza, A. O. S. Silva, V. J. Fernandes Jr. and A. S. Araujo, J. Therm. Anal. Cal., 79 (2005) 425.
21 H. L. Friedman, J. Polym. Sci, Part C, 6 (1964) 183.
22 J. Flynn and L.Wall, Polym. Lett., 5 (1967) 191.
23 S. J. Park and M. S. Cho, J. Mater. Sci., 35 (2000) 3525.
24 H. H. Horowitz and G. Metzger, Anal. Chem., 35 (1963) 1464.
25 T. Ozawa, Bull. Chem. Soc. Jpn., 38 (1965) 881.
26 V. M. Fonseca, V. J. Fernandes Jr., A. S. Araujo, L. H. Carvalho and A. G. Souza, J. Therm. Anal. Cal., 79 (2005) 429.
27 R. J. Jeng, S. M. Shau, J. J. Lin, W. C. Su and Y. S. Chiu, Eur. Polym. J., 38 (2002) 683.
28 J. Y. Shieh and C. S. Wang, Polymer, 42 (2001) 7617.
29 R. Barendregt and D. B. P. Van, Thermochim. Acta., 38 (1980) 181.
30 F. Gaboriaud and J. Vantelon, J. Polym. Sci. Polym. Chem., 20 (1982) 2063.
31 A. Ballistreri, S. Foti, P. Maravigna, G. Monaudo and E. Scamperrino, J. Polym. Sci. Pol. Chem., 18 (1980) 1923.
32 N. Grassie and D. Mackerron, Polym. Degrad. Stab., 5 (1983) 43.
33 Y. L. Liu, G. H. Hsiue, C. W. Lan and Y. S. Chiu, Polym. Degrad. Stab., 56 (1997) 291.
34 B. Wu, Y. Z. Wang, X. L. Wang, K. K. Yang, Y. D. Jin and H. Zhao, Polym. Degrad. Stab., 76 (2002) 401.

Received: February 22, 2006
Accepted: March 27, 2006
OnlineFirst: August 11, 2006

DOI: 10.1007/s10973-006-7552-z